The Canadian Mineralogist
Vol. 47, pp. 181-191 (2009)
DOI: 10.3749/canmin.47.1.181

LALONDEITE, A NEW HYDRATED Na–Ca FLUOROSILICATE SPECIES FROM MONT SAINT-HILAIRE, QUEBEC: DESCRIPTION AND CRYSTAL STRUCTURE

Andrew M. McDONALD[§]

Mineral Exploration Centre and Department of Earth Sciences, Laurentian University, Sudbury, Ontario P3E 2C6, Canada

George Y. CHAO[¶]

Ottawa–Carleton Geoscience Centre, Department of Earth Sciences, Carleton University, Ottawa, Ontario K1S 5B6, Canada

Abstract

Lalondeite, ideally $(Na,Ca)_6(Ca,Na)_3Si_{16}O_{38}(F,OH)_2{\bullet}3H_2O$, is a new mineral species from the Poudrette quarry, Mont Saint-Hilaire, Quebec. The mineral forms elongate aggregates of densely packed, randomly oriented crystals. Individual crystals are colorless, subhedral, roundish plates, typically measuring <0.5 mm in thickness and up to three mm across, dominated by the pinacoid {001}. Associated minerals include microcline, clinoamphibole and narsarssukite. The mineral has a vitreous luster, and is transparent with a white streak. It shows no fluorescence under long-wave ultraviolet radiation, a medium to strong violet-blue fluorescence under medium-wave radiation, and a weak violet to violet-blue fluorescence under short-wave radiation. It has a Mohs hardness of ~3, an inelastic, perfect {001} cleavage, and is brittle with a splintery fracture; its density is 2.50(1) (measured) and 2.51 g/cm^3 (calculated). Lalondeite is non-pleochroic, biaxial negative, with α 1.522(1), β 1.528(1), γ 1.529(1) (for $\lambda = 589$ nm), $2V_{meas} = 48(1)°$, $2V_{calc} = 44(1)°$; no dispersion was noted. The optical orientation is $X \approx c$. The average result of eighteen analyses of three crystals made using combined energy- and wavelength-dispersive spectrometries gave: Na_2O 11.28, K_2O 0.70, CaO 15.00, SiO_2 66.36, F 1.28, Cl 0.18 and H_2O (calc.) 4.27, O = F + Cl –0.58, total 98.49 wt.%. The empirical formula, based on 43 anions (O + F + Cl), is: $(Na_{5.33}Ca_{0.91}K_{0.22})_{\Sigma 6.46}Ca_3Si_{16.16}O_{38}(F_{0.99}OH_{0.94}Cl_{0.07})_{\Sigma 2}{\bullet}3H_2O$ or, ideally, $(Na,Ca,\square)_6Ca_3Si_{16}O_{38}(F,OH)_2{\bullet}3H_2O$. The mineral does not effervesce in 1:1 HCl at room temperature. The principal absorption bands in the infrared spectrum include 3443, 1631 and 1025 cm^{-1} (shoulder at 1121 cm^{-1}) with four bands in the region of 787–388 cm^{-1}. The mineral is triclinic, space group $P\bar{1}$, *a* 9.589(2), *b* 9.613(2), *c* 12.115(2) Å, α 96.62(2), β 92.95(2), γ 119.81(2)°, *V* 954.8(1) Å^3, *Z* = 2. The strongest seven lines in the X-ray powder-diffraction pattern [*d* in Å(*I*)(*hkl*)] are: 11.938(90)(001), 4.142(30)($2\bar{2}0$), 4.106(30)(020,$0\bar{2}1$), 3.972(40)(003,$1\bar{2}2$), 2.981(35)($2\bar{1}3$,004), 2.967(50)($\bar{1}\bar{2}2$,$3\bar{1}1$,$\bar{1}04$,$\bar{2}31$) and 2.888(100)($\bar{1}23$,121,$2\bar{3}2$,$\bar{3}12$). The crystal structure of lalondeite is strongly layered along [001], with sheets of tetrahedra (*T*) and octahedra (*O*). The *T* layers are composed of six-membered rings of SiO_4 tetrahedra cross-linked by SiO_4 tetrahedra, and the *O* layers contain edge-sharing $M\phi_{6-7}$ octahedra and polyhedra (*M*: Na,Ca; ϕ: unspecified ligand). The *O* sheets are sandwiched between two symmetrically equivalent *T* layers ($T_2,\bar{T}_2$), producing a strongly bonded *T–O–T* unit. The interlayer region houses disordered Na ions and H_2O molecules. Stacking of the principal components perpendicular to [001] results in a $OT_2\bar{T}_2O$ module, similar to that found in specific members of the reyerite–gyrolite group.

Keywords: lalondeite, new mineral species, layered fluorosilicate hydrate, reyerite–gyrolite group, crystal structure, Mont Saint-Hilaire, Quebec.

Sommaire

Nous décrivons la lalondeïte, de formule idéale $(Na,Ca)_6(Ca,Na)_3Si_{16}O_{38}(F,OH)_2{\bullet}3H_2O$, nouvelle espèce minérale provenant de la carrière Poudrette, au mont Saint-Hilaire, Québec. Le minéral se présente en longs groupements denses de cristaux orientés aléatoirement. Les cristaux individuels sont incolores, sub-idiomorphes, arrondis, minces (<0.5 mm en épaisseur) et jusqu'à 3 mm de diamètre, avec prédominance du pinacoïde {001}. Lui sont associés microcline, clinoamphibole et narsarssukite. Le minéral possède un éclat vitreux, et il est transparent avec une rayure blanche. Il ne montre aucune fluorescence en rayonnement ultraviolette à grande longueur d'onde, une fluorescence violette à bleue modérée à forte avec une longueur d'onde intermédiaire, et une faible fluorescence violette à violette-bleue avec une courte longueur d'onde. Sa dureté de Mohs est environ 3. Le clivage {001} est parfait, et les fragments sont cassants et inélastiques, avec une fracture hachée. Sa densité est 2.50(1) (mesurée) et 2.51 g/cm^3 (calculée). La lalondeïte est non pléochroïque, biaxe négative, avec α 1.522(1), β 1.528(1), γ 1.529(1) (λ = 589 nm), $2V_{mes}$

[§] *E-mail address*: amcdonald@laurentian.ca

[¶] *Present address*: 2031 Delmar Drive, Ottawa, Ontario K1H 5P6, Canada.

= 48(1)°, $2V_{calc}$ = 44(1)°, et sans dispersion apparente. L'orientation optique est X ≈ *c*. Le résultat moyen de dix-huit analyses de trois cristaux, en dispersion d'énergie et de longueurs d'onde, a donné: Na_2O 11.28, K_2O 0.70, CaO 15.00, SiO_2 66.36, F 1.28, Cl 0.18 et H_2O (calculé) 4.27, O = F + Cl –0.58, pour un total de 98.49% (poids). La formule empirique, fondée sur une base de 43 anions (O + F + Cl), est: $(Na_{5.33}Ca_{0.91}K_{0.22})_{\Sigma 6.46}Ca_3Si_{16.16}O_{38}(F_{0.99}OH_{0.94}Cl_{0.07})_{\Sigma 2}\bullet 3H_2O$ ou, de façon idéale, $(Na,Ca,\square)_6Ca_3Si_{16}O_{38}(F,OH)_2\bullet 3H_2O$. Il n'y a aucune effervescence à l'acide 1:1 HCl à température ambiante. Parmi les bandes d'absorption principales du spectre infrarouge figurent celles à 3443, 1631 and 1025 cm^{-1} (épaulement à 1121 cm^{-1}) et, en plus, quatre bandes dans la région 787–388 cm^{-1}. Il s'agit d'un minéral triclinique, groupe spatial $P\overline{1}$, *a* 9.589(2), *b* 9.613(2), *c* 12.115(2) Å, α 96.62(2), β 92.95(2), γ 119.81(2)°, *V* 954.8(1) $Å^3$, *Z* = 2. Les sept raies les plus intenses du spectre de diffraction (méthode des poudres) [*d* en Å(*I*)(*hkl*)] sont: 11.938(90)(001), 4.142(30)($2\overline{2}0$), 4.106(30)(020,$0\overline{2}1$), 3.972(40)(003,$1\overline{2}2$), 2.981(35)($2\overline{1}3$,004), 2.967(50)($\overline{1}22$,$3\overline{1}1$,04,$\overline{2}31$) et 2.888(100)($\overline{1}23$,121,$2\overline{3}2$,$\overline{3}12$). La structure de la lalondeïte est fortement stratifiée selon [001], avec des feuillet de tétraèdres (*T*) et d'octaèdres (*O*). Les feuillets *T* contiennent des anneaux de six tétraèdres SiO_4 avec connexions entre anneaux assurées par des tétraèdres SiO_4, et les couches *O* contiennent des octaèdres $M\phi_{6-7}$ à arêtes partagées et des polyèdres (*M*: Na,Ca; ϕ: ligand non spécifié). Chaque feuillet *O* est intercalé entre deux feuillets *T* symétriquement équivalents ($T_2,\overline{T}_2$), avec comme résultat une unité *T–O–T* à liaisons fortes. Les ions Na désordonnés et les molécules de H_2O logent dans la région interfoliaire. L'empilement des composants principaux perpendiculaire à [001] mène à un module $OT_2\overline{T}_2O$, semblable à ceux qui caractérisent les divers membres du groupe de la reyerite–gyrolite.

(Traduit par la Rédaction)

Mots-clés: lalondeïte, nouvelle espèce minérale, fluorosilicate hydraté stratifié, groupe de la reyerite–gyrolite, structure cristalline, mont Saint-Hilaire, Québec.

INTRODUCTION

Minerals of the reyerite–gyrolite group are strongly layered alkali and alkaline-earth silicate hydrate phases possessing trigonal or strongly pseudotrigonal symmetry. Most are considered to be late-stage products, developing by low-temperature alteration or low-grade metamorphism of alkali-rich igneous rocks. In this paper, we describe the eighth and newest member of the group, lalondeite, ideally $(Na,Ca)_6(Ca,Na)_3Si_{16}O_{38}(F,OH)_2\bullet 3H_2O$. When first noticed, the mineral was considered to be a colorless phyllosilicate, possibly muscovite or phlogopite. However, combined X-ray diffraction and qualitative chemical analyses suggested it to be a new Na–Ca fluorosilicate hydrate. It was temporarily designated UK57 (Wight & Chao 1995). Lalondeite represents the second new member of the reyerite–gyrolite group discovered at Mont Saint-Hilaire, Quebec, the other being martinite (McDonald & Chao 2007). The new mineral is named after Prof. André Edmond Lalonde (*b*. 1955), Professor of Geology at the University of Ottawa, Ottawa, Ontario, Canada, in recognition of his work on the mineralogy of micas and the petrology of alkaline intrusions. The mineral and mineral name have been approved by the Commission on New Minerals and Mineral Names, IMA (IMA 2002–026). The holotype material is housed in the collection of the Canadian Museum of Nature, Aylmer, Quebec, Canada (catalogue no. CMNMC 83720). A second sample containing lalondeite from Mont Saint-Hilaire has been recognized in a similar suite of samples (CMNMC 83717), although no specific details concerning its collection are known.

In this paper, we characterize the new species, resolve details of its crystal-structure arrangement, and comment on its relationship to other members of the reyerite–gyrolite group.

OCCURRENCE

Lalondeite was first discovered on a single, hand-sized sample of altered breccia (or possibly, altered marble) collected in the summer of 1985 at the Poudrette quarry, Mont Saint-Hilaire, Rouville County, Quebec (Fig. 1). The sample was not found *in situ*, making it difficult to unequivocally classify the microenvironment from which it came. Lalondeite is rather abundant on the sample, perhaps representing up to two percent by volume. The mineral forms elongate aggregates of crystals that are densely packed and randomly oriented. Associated minerals include microcline, clinoamphibole and narsarssukite. The type sample is distinctly light green in color, suggesting a rather high modal concentration of clinoamphibole.

PHYSICAL AND OPTICAL PROPERTIES

Crystals of lalondeite occur as subhedral, roundish plates typically measuring <0.5 mm in thickness and up to three mm across. The crystals, dominated by the pinacoid {001} (no other forms noted) are colorless. No twinning was observed by optical microscopy or by single-crystal X-ray-diffraction methods. The mineral has a pearly luster, a white streak, and is transparent. The mineral shows no fluorescence in long-wave radiation (λ = 368 nm), a medium to strong violet-blue fluorescence under medium-wave radiation (λ = 312 nm), and a weak violet to violet-blue fluorescence under short-wave radiation (λ = 254 nm). It has a Mohs hardness of ~3, a perfect {001} cleavage, and is brittle with a splintery fracture. Consistent with other members of the reyerite–gyrolite group, cleavage fragments of lalondeite are inelastic, making this a characteristic useful for distinguishing it from similar-looking colorless micas. The density, measured using the sink–float method, is 2.50(1) g/cm^3, which compares well with the value of 2.51 g/cm^3 calculated from the empirical formula and the unit-cell dimensions derived from the crystal-structure analysis.

Lalondeite is non-pleochroic, biaxial negative, with α 1.522(1), β 1.528(1), γ 1.529(1) (for λ = 589 nm), $2V_{\text{meas}}$ = 48(1)°, $2V_{\text{calc}}$ = 44(1)°; no dispersion was noted. The optical orientation is $X \approx c$. A Gladstone–Dale calculation gave a compatibility index of –0.002, which is classed as superior (Mandarino 1981).

CHEMICAL COMPOSITION

Chemical analyses were conducted on a CAMEBAX SX50 electron microprobe using an operating voltage of 15 kV, a beam current of 10 nA and a beam diameter of approximately 10 μm. Owing to rather severe decrepitation, the electron beam was moved 10 μm after every 5 s of beam exposure. Energy-dispersion data were collected using Kakanui hornblende as a standard. In addition, wavelength-dispersion data were collected using the same standard, for Na, F and Cl. No other elements were indicated in qualitative EDS scans. Also sought, but not detected, are Al, Ti, Fe, Mg, Rb and Cs. Eighteen analyses of three crystals gave as an average (range): Na_2O 11.28 (10.06 – 11.99), K_2O 0.70 (0.49 – 0.77), CaO 15.00 (14.82 – 15.20), SiO_2 66.36 (65.64 – 67.38), F 1.28 (1.10 – 1.51), Cl 0.18 (0.14 – 0.21) and H_2O (calc.) 4.27, O = F+Cl –0.58, total 98.49 wt.%. The presence of H_2O was confirmed by infrared spectroscopy (see below) and results from the crystal-structure analysis. The empirical formula, based on 43 anions (O + F + Cl), is: $(Na_{5.33}Ca_{0.91}K_{0.22})_{\Sigma 6.46}Ca_3Si_{16.16}O_{38}(F_{0.99}OH_{0.94}Cl_{0.07})_{\Sigma 2}\bullet 3H_2O$ or, ideally, $(Na,Ca)_6Ca_3Si_{16}O_{38}(F,OH)_2\bullet 3H_2O$. The mineral does not effervesce in 1:1 HCl at room temperature.

INFRARED ANALYSIS

The infrared spectrum of lalondeite (Fig. 2) was obtained using a Bomem Michelson MB–120 Fourier transform infrared spectrometer equipped with a mercury–cadmium telluride (MCT) detector. A single crystal of material was mounted in a Spectra-Tech low-pressure diamond-anvil microsample cell. The spectrum, in fact a sum of 200 co-added scans, was obtained over the range 4000 – 400 cm^{-1}. Absorption bands were assigned using data from Farmer (1974). The spectrum shows a broad band centered at the 3443 cm^{-1} region (O–H stretching), and a relatively weak, broad band at 1631 cm^{-1} (H–O–H bending). The spectrum also shows a strong, sharp band at 1025 and a shoulder at 1121 cm^{-1} (asymmetric O–Si–O stretching), along with four sharp, weak to moderately strong bands in the region 787 – 388 cm^{-1} (symmetric Si–O–Si stretching; Farmer 1974). Based on the observed absorption bands, the spectrum is very similar to that of the related species, martinite.

X-RAY CRYSTALLOGRAPHY AND CRYSTAL-STRUCTURE DETERMINATION

The X-ray powder-diffraction data (Table 1) were collected with a Debye–Scherrer camera 114.6 in diameter, employing Ni-filtered Cu$K\alpha$ radiation (λ = 1.5418 Å). Interplanar spacing and intensity data were determined using a scanned X-ray film. Whether or not an *hkl* plane contributed to a reflection was determined from the powder pattern calculated using the atomic parameters determined in the crystal-structure analysis and the program POWDERCELL (Nolze & Kraus 1998).

A single crystal mounted approximately parallel to c^* was used for the collection of X-ray intensity data. These were collected on a fully automated Enraf–Nonius CAD4 four-circle diffractometer operated at 50 kV, 26 mA, with graphite-monochromated Mo$K\alpha$ radiation. It should be noted that the unit cell given herein has been transformed from that originally referenced (IMA #2002–026, so as to adhere to the IUCr convention, $c < a < b$), in order to emphasize the relationship between lalondeite and minerals of the reyerite–gyrolite group. A full sphere of X-ray intensity data out to 2θ = 55.1° was collected using a θ–2θ scan-mode, with scan speeds inversely proportional to intensity. With these operating conditions, no decrepitation was evident in the final analysis of the reflections used as intensity standards. Data measurement and reduction (Lorentz, polarization, background, scaling) were carried out using the NRCVAX set of computer programs (Gabe *et al.* 1989). No absorption correction was applied to the data given the low μ value of the mineral. Information pertinent to the data collection and structure determination is provided in Table 2.

Solution and refinement of the crystal structure were accomplished using the SHELX–93 package of programs (Sheldrick 1993). The crystal structure was solved using direct methods, with scattering curves and anomalous dispersion coefficients taken from Cromer & Mann (1968) and Cromer & Liberman (1970), respectively. Preliminary X-ray precession photographs indicated P^* diffraction symmetry. Phasing of a set of normalized structure-factors gave a mean value of $|E^2 - 1|$ equal to 0.972 (predicted values: 0.968, centrosymmetric, 0.736, non-centrosymmetric). On this basis, $P\overline{1}$ was selected and proved to be the correct space-group. Phase-normalized factors were calculated and used to produce an E-map on which were located *Ca* sites, along with several *Si* and *O* sites. The remaining *Na* and *O* sites were located on subsequent Fourier-difference

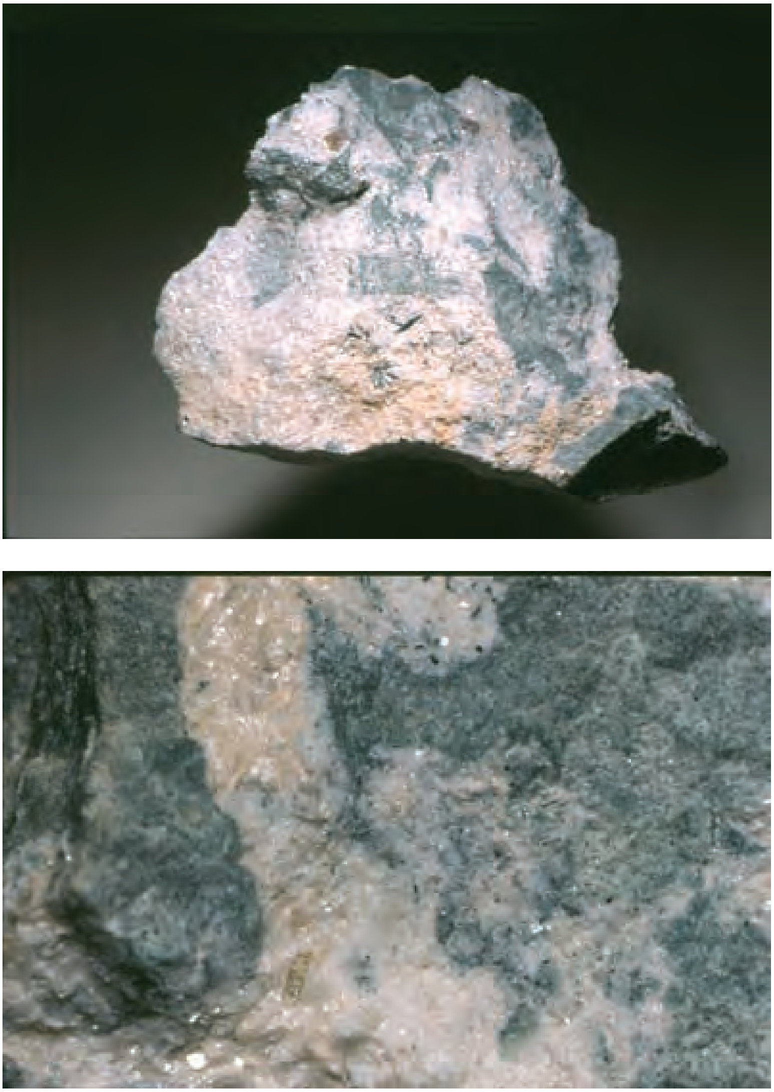

FIG. 1. A. A sample of lalondeite with a clinoamphibole (greenish). The field of view is approximately 10 cm across (CMN #83717). B. Closeup of a vein of lalondeite; the field of view is approximately 3 cm across. Photographs by L. Horváth.

maps. Anisotropic refinement of this model indicated that the *Na1* and *Ca3* sites have lower-than-ideal site-occupancy factors (*sof*; Table 3). An attempt at refining the *Na1* with a mixed (Na,Ca) occupancy was not successful, and the assumption was thus made that this site is partially vacant. A similar process with the *Ca3* site indicated an almost equal proportion of Ca and Na, with the refined result being indicated in Table 3. The *Na2* site was found to exhibit a pronounced thermal displacement anisotropy along *c* and was subsequently refined as a split site. Determination of those *O* sites likely occupied by H_2O was made on the basis of bond-valence calculations in conjunction with charge-balance considerations. Refinement of the anisotropic thermal displacements factors for the three H_2O groups identified in this manner were found to produce illogical results; for that reason, the refinement was fixed to be isotropic. Finally, as lalondeite contains essential F, one site was identified as being the probable host on the basis of bond-valence considerations, and was thus assumed to be fully occupied by F. Final least-squares refinement of this model gave residuals of $R = 3.29$ and

wR^2 = 7.24%, with maximum and minimum electron-densities of +2.55 and –1.69 $e/\text{Å}^3$. Refinement of this model indicated that several of the ions display non-positive definite behavior (*Na*2b, *O*4, *O*5, *O*12, *O*17), although the extent of this behavior was not deemed to be excessive for any of the ions involved.

Table 3 contains the final positional and displacement parameters, with selected interatomic distances in Table 4, and bond-valence sums in Table 5. Observed and calculated structure-factors have been submitted to the Depository of Unpublished Data on the MAC website [document Lalondeite CM47_181].

DESCRIPTION OF THE CRYSTAL STRUCTURE

The crystal structure of lalondeite (Fig. 3) is similar to that of other members of the reyerite–gyrolite group. It is strongly layered perpendicular to [001], and consists of sheets of tetrahedra (*T*), octahedra (*O*) and interlayer cations (*X*). The *T* layers (specifically, T_2, using the terminology of Merlino 1988) are composed of six-membered pseudohexagonal rings of SiO_4 tetrahedra that are linked by bridging tetrahedra ($\mathit{Si}3\mathrm{O}_4$, $\mathit{Si}6\mathrm{O}_4$) in the *a–b* plane to complete the sheet. The apices of SiO_4 tetrahedra in the rings all point in a common direction, toward the *O* sheet ([001]), but deviate slightly away from [001], owing to geometrical restrictions resulting from linkages made with overlying *O* sheets. This deviation contributes to a reduction in the overall symmetry of the mineral, although a strong pseudohexagonal character is retained. The two crystallographically distinct bridging tetrahedra that interconnect the pseudohexagonal silicate rings in the *a–b* plane, $\mathit{Si}3\mathrm{O}_4$ and $\mathit{Si}6\mathrm{O}_4$, are oriented such that their apices point away from the *O* sheets, toward the discontinuous interlayer region of the structure. The two tetrahedra are directly linked to one another along [001] through a common apical oxygen, *O*4, a situation similar to that observed in fedorite (Mitchell & Burns 2001).

Four distinct cations *Na*1, (*Ca*,*Na*)3, and *Ca*2, in general positions, and *Ca*1 in a special position at the inversion center, occur in the sheets of octahedra (*O*). The *O* sheets consist of a closest-packed arrangement of seven edge-sharing $M\phi_{6-7}$ octahedra and polyhedra (*M*: Na,Ca; ϕ: unspecified ligand). These sheets are joined to the T_2 layers through apical atoms of oxygen from the SiO_4 tetrahedra of the pseudohexagonal rings. The *O* sheets are effectively sandwiched between two

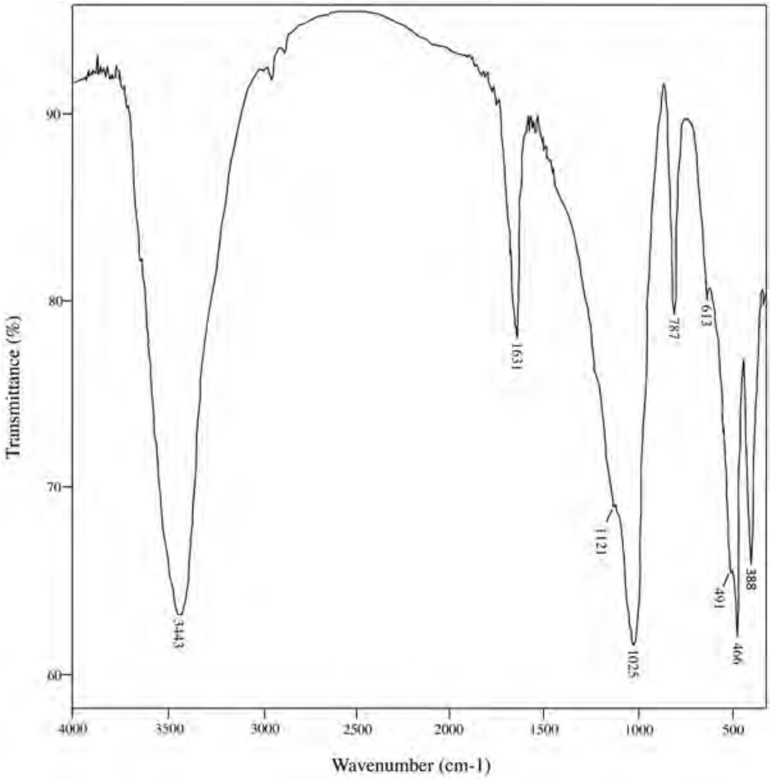

FIG. 2. Infrared spectrum of lalondeite.

symmetrically equivalent T_2 layers (T_2,$\overline{T_2}$), producing a strongly bonded *T–O–T* unit. As noted, the bridging SiO_4 tetrahedra (*i.e.*, those tetrahedra not part of the six-membered rings of SiO_4 tetrahedra) have their apical directions oriented along [001], away from the *T–O–T* unit and toward a discontinuous interlayer component (*i.e.*, it is bisected by the bridging *Si*3O_4 and *Si*6O_4 tetrahedra) that houses poorly ordered (*Na*2a,2b)–O polyhedra and H_2O molecules. If viewed along [001], the H_2O molecules of the interlayer region are found to decorate the peripheries of the six-membered SiO_4 rings, with the (*Na*2a,2b)–O polyhedra being positioned

TABLE 1. LALONDEITE: X-RAY POWDER-DIFFRACTION DATA

I_{meas}	I_{calc}	d_{obs}	d_{calc}	*h*	*k*	*l*
90	100	11.987	11.938	0	0	1
25	8	8.306	8.301	1	$\bar{1}$	0
85	66	5.968	5.969	0	0	2
10	3	4.776	4.774	1	$\bar{2}$	0
			4.763	$\bar{1}$	1	2
10	3	4.691	4.687	$\bar{1}$	$\bar{1}$	1
5	3	4.521	4.526	$\bar{2}$	1	1
5	5	4.363	4.366	2	$\bar{1}$	1
5	3	4.249	4.266	$\bar{1}$	2	1
30	10	4.142	4.150	2	$\bar{2}$	0
30	8	4.106	4.115	0	2	0
	5		4.101	0	$\bar{2}$	1
10	9	4.055	4.062	$\bar{2}$	0	1
	6		4.056	$\bar{1}$	$\bar{1}$	2
40	11	3.972	3.979	0	0	3
	10		3.958	1	$\bar{2}$	2
10	7	3.825	3.833	$\bar{2}$	1	2
5	3	3.654	3.644	2	$\bar{1}$	2
	3		3.641	1	$\bar{1}$	3
5	7	3.621	3.615	$\bar{2}$	0	2
5	5	3.469	3.468	2	$\bar{2}$	2
10	3	3.355	3.350	$\bar{2}$	2	2
1	3	3.248	3.247	1	$\bar{2}$	3
20	4	3.139	3.140	$\bar{1}$	$\bar{2}$	1
	2		3.138	3	$\bar{2}$	0
	4		3.130	3	$\bar{1}$	0
30	2	3.112	3.111	1	$\bar{3}$	0
	7		3.107	1	2	0
	8		3.098	2	$\bar{3}$	1
	8		3.090	$\bar{3}$	1	1
5	1	3.050	3.050	$\bar{3}$	2	1
35	7	2.981	2.985	2	$\bar{1}$	3
	13		2.984	0	0	4
50	4	2.967	2.971	$\bar{1}$	$\bar{2}$	2
	4		2.968	3	$\bar{1}$	1
	1		2.964	0	$\bar{1}$	4
	4		2.964	$\bar{2}$	3	1
100	12	2.888	2.896	$\bar{1}$	2	3
	25		2.889	1	2	1
	26		2.881	2	$\bar{3}$	2
	26		2.870	$\bar{3}$	1	2
10	9	2.831	2.827	1	1	3
10	5	2.780	2.774	0	$\bar{3}$	1
10	3	2.763	2.767	3	$\bar{3}$	0
	3		2.758	$\bar{3}$	0	1
10	7	2.735	2.740	$\bar{1}$	$\bar{1}$	4
20	2	2.691	2.700	2	0	3
	2		2.683	3	$\bar{1}$	2
	2		2.680	$\bar{1}$	$\bar{2}$	3
	2		2.676	$\bar{2}$	3	2
20	5	2.589	2.594	$\bar{2}$	1	4
	4		2.582	1	2	2
10	4	2.568	2.576	2	$\bar{3}$	3
	3		2.564	$\bar{3}$	1	3
1	1	2.486	2.488	$\bar{3}$	2	3
1	2	2.470	2.476	2	$\bar{1}$	4
10	2	2.407	2.406	$\bar{2}$	$\bar{2}$	1
5	1	2.366	2.368	3	$\bar{1}$	3
1	1	2.306	2.309	1	$\bar{4}$	1
	1		2.308	$\bar{3}$	$\bar{1}$	1
10	2	2.267	2.269	1	2	3
5	1	2.143	2.152	$\bar{4}$	3	2
			2.145	4	$\bar{3}$	2
			2.142	$\bar{1}$	$\bar{3}$	3
1	1	2.127	2.123	$\bar{3}$	$\bar{1}$	3
	1		2.121	1	$\bar{4}$	3
1	1	2.074	2.075	4	$\bar{4}$	0
	1		2.071	$\bar{1}$	$\bar{2}$	5
5	1	2.042	2.056	$\bar{2}$	$\bar{1}$	5
	1		2.039	$\bar{1}$	4	2
10	2	1.991	1.990	1	2	4
10	2	1.983	1.986	4	$\bar{4}$	2
	1		1.982	$\bar{1}$	$\bar{3}$	4
	2		1.978	$\bar{3}$	1	5
1	1	1.958	1.961	$\bar{3}$	$\bar{1}$	4
	5		3.131	2	$\bar{3}$	0
	1		1.954	1	$\bar{1}$	6
15	1	1.916	1.919	$\bar{1}$	1	6
	2		1.917	1	$\bar{2}$	6
	2		1.912	$\bar{3}$	$\bar{2}$	1
	1		1.911	4	$\bar{1}$	3
	1		1.910	2	$\bar{5}$	1
50	10	1.820	1.819	1	$\bar{5}$	1
	10		1.817	$\bar{4}$	4	1
	10		1.812	5	$\bar{4}$	0
15	1	1.800	1.804	2	$\bar{1}$	6
	1		1.799	1	$\bar{5}$	0
	1		1.798	1	$\bar{5}$	2
	1		1.798	4	1	0
	1		1.795	$\bar{4}$	$\bar{1}$	2
1	1	1.762	1.766	$\bar{1}$	2	6
	1		1.766	4	$\bar{5}$	2
	1		1.758	5	$\bar{1}$	1
5	1	1.703	1.705	0	0	7
10	1	1.657	1.657	$\bar{5}$	2	4
	1		1.654	4	$\bar{3}$	5
10	1	1.620	1.623	2	$\bar{4}$	6
	1		1.623	1	$\bar{4}$	6
	1		1.620	3	$\bar{1}$	6
	2		1.619	$\bar{5}$	1	4
1	1	1.602	1.607	$\bar{4}$	5	3
	1		1.596	4	$\bar{5}$	4
10	1	1.538	1.539	2	$\bar{4}$	3
	1		1.536	6	$\bar{2}$	1
	1		1.535	$\bar{6}$	$\bar{1}$	4
15	2	1.4908	1.4922	0	0	8
15	2	1.4456	1.4445	$\bar{1}$	$\bar{2}$	8
	2		1.4442	$\bar{2}$	3	7
1	1	1.3823	1.3835	6	$\bar{6}$	0
1	1	1.3527	1.3539	1	$\bar{6}$	5
15	2	1.3329	1.3341	$\bar{2}$	$\bar{5}$	2
	2		1.3310	5	$\bar{7}$	1
	2		1.3304	$\bar{7}$	2	1
1	2	1.3278	1.3264	0	0	9
5	1	1.3039	1.3061	3	$\bar{1}$	8
	1		1.3049	6	0	2
	1		1.3045	7	$\bar{2}$	1

The values of *d* are reported in Å.

in the center of these rings. The (*Na*2a,2b)–O polyhedra alternate with *F* ions in the center of these same rings, and are repeated by the center of symmetry. Bonding between the H_2O molecules and the (*Na*2a,2b)–O polyhedra in the interlayer component and the adjacent T_2 sheets is weak, likely involving considerable H-bonding (although the intensity data were not of sufficient resolution to discern H positions), presumably resulting in the perfect {001} cleavage observed in the mineral. Further, as observed in the related species martinite, cleavage fragments of lalondeite have an inelastic, brittle nature that can be explained by the presence of Na polyhedra of low coordination in the *X* layer, producing an interlayer of quasi-octahedra, similar to that found in brittle micas or in chlorite-group minerals.

TABLE 2. MISCELLANEOUS INFORMATION FOR LALONDEITE

Space group	$P\bar{1}$	Diffractometer	Enraf Nonius CAD4
a (Å)	9.589(2)*	Radiation	Mo*K*α (50 kV, 26 mA)
b	9.613(2)*	Monochromator	Graphite
c	12.115(2)*	Crystal shape	Plate flattened on [001]
α (°)	96.62(2)*	Crystal size	0.025 × 0.2 × 0.25 mm
β	92.95(2)*	μ(Mo*K*α)	1.15 mm^{-1}
γ	119.81(2)*	*Z*	2
V ($Å^3$)	954.8(1)		
Chemical Formula	$(Na,Ca,\square)_6Ca_3Si_{16}O_{38}(F,OH)_2\cdot 3H_2O$		
Intensity-data collection	θ:2θ scan mode		
2θ limit	55.1°		
Number of unique reflections	1009		
Number of observed reflections	761		
Criterion for observed reflections	$F_o > 4\sigma(F_o)$		
GoOF	1.027		
Final *R* for all observed reflections (%)	3.29		
Final wR^2 for observed reflections (%)	7.24		

* Values were refined from four-circle diffractometer data.

TABLE 3. POSITIONAL AND DISPLACEMENT PARAMETERS FOR LALONDEITE

	x	*y*	*z*	sof	U_{11}	U_{22}	U_{33}	U_{23}	U_{13}	U_{12}	U_{eq}
Na1	0.1377(7)	0.9294(6)	0.9990(8)	0.82(2)	0.024(3)	0.022(3)	0.041(8)	0.014(5)	0.004(4)	0.009(2)	0.029(4)
Na2a	0.041(2)	0.052(2)	0.714(3)	0.50(6)	0.014(7)	0.018(7)	0.09(3)	0.03(1)	0.021(9)	0.011(5)	0.037(10)
Na2b	0.979(5)	0.976(5)	0.361(9)	0.50(6)	0.07(2)	0.08(2)	0.00(6)	-0.04(3)	-0.01(3)	0.03(2)	0.06(2)
Ca1	0	½	0	1.00	0.007(1)	0.011(1)	0.006(3)	0.000(2)	0.002(2)	0.003(1)	0.008(1)
Ca2	0.4258(2)	0.7878(2)	0.9952(2)	1.00	0.074(7)	0.0085(8)	0.011(2)	0.002(1)	-0.001(1)	0.028(7)	0.0096(9)
Ca3	0.2944(3)	0.3648(3)	0.0129(3)	0.52(4)	0.014(2)	0.023(2)	0.022(4)	0.011(2)	0.004(2)	0.011(1)	0.018(2)
Na3				0.48(4)							
Si1	0.1909(3)	0.8038(3)	0.2244(3)	1.00	0.002(1)	0.007(1)	0.006(4)	0.001(2)	0.000(2)	0.001(1)	0.006(2)
Si2	0.1802(3)	0.4380(3)	0.7737(4)	1.00	0.004(1)	0.010(1)	0.012(4)	0.005(2)	0.003(2)	0.004(1)	0.008(1)
Si3	0.3050(3)	0.6306(3)	0.3632(4)	1.00	0.005(1)	0.010(2)	0.010(5)	0.005(3)	0.001(2)	0.003(1)	0.008(2)
Si4	0.3013(3)	0.9389(3)	0.7712(3)	1.00	0.006(1)	0.006(2)	0.007(4)	0.001(2)	0.001(2)	0.003(1)	0.006(2)
Si5	0.0729(3)	0.3070(3)	0.2256(4)	1.00	0.005(1)	0.008(1)	0.008(4)	0.001(3)	0.001(2)	0.003(1)	0.007(2)
Si6	0.3628(3)	0.6988(4)	0.6305(4)	1.00	0.005(1)	0.009(1)	0.006(5)	0.002(3)	0.000(2)	0.002(1)	0.007(2)
Si7	0.4236(3)	0.3067(3)	0.7753(3)	1.00	0.007(1)	0.009(1)	0.008(4)	0.003(2)	0.002(2)	0.005(1)	0.008(2)
Si8	0.3195(3)	0.1792(3)	0.2284(3)	1.00	0.006(1)	0.008(1)	0.012(4)	0.003(2)	0.000(2)	0.003(1)	0.009(1)
O1	0.0796(9)	0.3482(9)	0.1035(11)	1.00	0.016(4)	0.026(5)	0.02(1)	0.011(8)	0.007(5)	0.014(4)	0.018(5)
O2	0.5004(10)	0.3651(10)	0.9007(11)	1.00	0.026(5)	0.026(5)	0.03(1)	0.014(9)	0.003(7)	0.017(4)	0.025(5)
O3	0.9922(9)	0.2945(8)	0.7426(11)	1.00	0.002(4)	0.019(4)	0.04(1)	0.012(7)	0.000(5)	0.000(3)	0.022(5)
O4	0.335(1)	0.663(1)	0.496(2)	1.00	0.020(6)	0.021(7)	0.00(3)	-0.02(2)	0.005(10)	0.009(6)	0.016(10)
O5	0.2202(10)	0.5295(10)	0.899(1)	1.00	0.011(5)	0.014(4)	0.00(1)	-0.012(8)	-0.008(6)	0.002(4)	0.013(5)
O6	0.3786(9)	0.9582(8)	0.8944(8)	1.00	0.019(4)	0.010(4)	0.004(10)	-0.004(6)	-0.004(5)	0.007(3)	0.012(4)
O7	0.1811(8)	0.2253(8)	0.2551(9)	1.00	0.006(4)	0.016(3)	0.02(1)	0.005(6)	0.000(5)	0.007(3)	0.014(4)
O8	0.2070(10)	0.7491(10)	0.101(1)	1.00	0.020(5)	0.017(4)	0.02(2)	0.003(9)	0.016(6)	0.009(4)	0.019(6)
O9	0.3665(10)	0.2020(9)	0.1075(10)	1.00	0.018(4)	0.029(4)	0.02(1)	0.016(7)	0.009(6)	0.015(4)	0.022(5)
O10	0.3010(8)	0.7819(7)	0.3207(10)	1.00	0.007(4)	0.009(3)	0.02(1)	0.004(6)	-0.001(5)	0.003(3)	0.012(4)
O11	0.3332(10)	0.1099(8)	0.7363(10)	1.00	0.021(5)	0.013(3)	0.02(1)	0.005(6)	0.007(5)	0.012(3)	0.015(4)
O12	0.1356(9)	0.4647(8)	0.323(1)	1.00	0.006(4)	0.004(3)	0.01(1)	-0.012(7)	-0.004(5)	-0.001(3)	0.009(4)
O13	0.3685(10)	0.8670(8)	0.674(1)	1.00	0.016(5)	0.008(3)	0.02(2)	-0.002(8)	0.006(6)	0.005(3)	0.015(6)
O14	0.2148(8)	0.5525(8)	0.6774(9)	1.00	0.010(4)	0.013(3)	0.005(10)	0.004(6)	0.004(5)	0.004(3)	0.010(4)
O15	0.8952(9)	0.1736(8)	0.2498(10)	1.00	0.008(4)	0.021(4)	0.04(1)	0.012(7)	0.008(5)	0.007(3)	0.021(5)
O16	0.4503(8)	0.6150(7)	0.3166(8)	1.00	0.011(4)	0.011(3)	0.017(10)	0.005(6)	0.006(4)	0.006(3)	0.013(4)
O17	0.5327(8)	0.7132(8)	0.6708(10)	1.00	0.007(4)	0.010(3)	0.02(1)	-0.008(6)	-0.012(5)	0.001(3)	0.016(5)
O18	0.2367(10)	0.9926(8)	0.2519(10)	1.00	0.022(5)	0.010(3)	0.02(1)	0.001(6)	-0.008(6)	0.006(3)	0.019(4)
O19	0.2800(9)	0.3443(8)	0.7488(10)	1.00	0.013(4)	0.020(4)	0.03(1)	0.010(7)	-0.001(5)	0.011(3)	0.022(5)
F	0.090(1)	0.112(1)	0.912(2)	1.00	0.026(7)	0.048(7)	0.04(2)	0.01(1)	0.002(8)	0.009(5)	0.042(8)
OW20	0.365(5)	0.022(4)	0.490(5)	0.5							0.067(6)
OW21	0.990(9)	0.325(7)	0.504(9)	0.5							0.097(9)
OW22	0.692(7)	0.659(6)	0.497(9)	0.5							0.099(9)

TABLE 4. SELECTED INTERATOMIC DISTANCES (Å) IN LALONDEITE

	Na(1)Φ_7 polyhedron			Na(2)aΦ_7 polyhedron	
Na1	– F	2.36(2)	Na2a	– F	2.36(4)
	– F'	2.359(7)		– O7	2.54(1)
	– O1	2.54(1)		– O18	2.55(1)
	– O8	2.554(6)		– O11	2.56(1)
	– O9	2.57(1)		– O19	2.56(1)
	– O6	2.60(1)		– O3	2.59(2)
	– O15	3.01(1)		– O15	2.60(1)
<Na1	– Φ>	2.57	<Na2a	– Φ>	2.54
	Na(2)bO$_6$ polyhedron			[(Ca,Na)](3)Φ_6 octahedron	
Na2b	– O7	2.73(5)	(Ca,Na)3	– O1	2.33(1)
	– O18	2.80(6)		– F	2.36(2)
	– O11	2.82(5)		– O9	2.378(4)
	– O15	2.84(4)		– O2	2.41(1)
	– O3	2.90(6)		– O2'	2.46(1)
	– O19	2.92(6)		– O5	2.534(5)
<Na2b	– O>	2.84	<(Ca,Na)	– Φ>	2.41
	Ca(1)O$_6$ octahedron			Ca(2)O$_6$ octahedron	
Ca1	– O8 ×2	2.35(1)	Ca2	– O6	2.350(4)
	– O1 ×2	2.390(4)		– O9	2.37(1)
	– O5 ×2	2.40(1)		– O2	2.371(5)
<Ca1	– Φ>	2.38		– O5	2.37(1)
				– O6'	2.388(9)
				– O8	2.41(1)
			<Ca2	– O>	2.37
	Si(1)O$_4$ tetrahedron			Si(2)O$_4$ tetrahedron	
Si1	– O8	1.57(1)	Si2	– O5	1.59(1)
	– O3	1.626(8)		– O3	1.622(8)
	– O18	1.628(7)		– O19	1.625(8)
	– O10	1.634(8)		– O14	1.629(6)
<Si1	– O>	1.61	<Si2	– O>	1.62
	Si(3)O$_4$ tetrahedron			Si(4)O$_4$ tetrahedron	
Si3	– O4	1.58(2)	Si4	– O6	1.580(9)
	– O16	1.598(9)		– O13	1.61(1)
	– O12	1.607(9)		– O15	1.627(8)
	– O10	1.614(4)		– O11	1.628(4)
<Si3	– O>	1.60	<Si4	– O>	1.61
	Si(5)O$_4$ tetrahedron			Si(6)O$_4$ tetrahedron	
Si5	– O1	1.57(1)	Si6	– O17	1.609(7)
	– O15	1.612(8)		– O4	1.61(3)
	– O7	1.630(5)		– O14	1.613(7)
	– O12	1.63(1)		– O13	1.616(8)
<Si5	– O>	1.61	<Si6	– O>	1.61
	Si(7)O$_4$ tetrahedron			Si(8)O$_4$ tetrahedron	
Si7	– O2	1.56(1)	Si8	– O9	1.56(1)
	– O19	1.615(6)		– O17	1.63(1)
	– O11	1.635(8)		– O18	1.629(5)
	– O16	1.641(8)		– O7	1.630(8)
<Si7	– O>	1.61	<Si8	– O>	1.61

RELATED PHASES

Lalondeite is the newest member of the reyerite–gyrolite group (Bonaccorsi & Merlino 2005, McDonald & Chao 2007), which consists of a number of layered alkali and alkaline-earth silicate and aluminosilicate hydrates having a trigonal or strongly pseudotrigonal symmetry (Table 6). The crystal structures of these phases contain sheets of octahedra (*O*), tetrahedra (*T*), a variety of interlayer components (*X*), along with symmetry equivalents of all three (indicated by a "bar" *e.g.*, $\overline{O}$), using the terminology of Merlino (1988). The sheets of octahedra are all closest-packed (brucite-like) and occupied either solely by Ca or by a combination of Ca, Na or Mn. Two different sheets of tetrahedra may be present in minerals belonging to this group, each with the composition T_8O_{20} (*T*: tetrahedrally coordinated cation, Si, Al, B or S). The first sheet, termed T_1, has four tetrahedra whose vertices point in one direction and four tetrahedra with vertices pointing in the opposite direction, this sheet being connected to sheets of octahedra (*O*) on both sides. The second sheet, termed T_2, has six tetrahedra whose vertices point in one direction (toward a sheet of octahedra) and two whose vertices point in the other. All members of the reyerite–gyrolite group possess T_2 layers of tetrahedra, although only some members possess *both* T_1 and T_2 layers (*e.g.*, reyerite itself).

The T_2 layers present in phases belonging to the reyerite–gyrolite group may or may not be condensed through shared vertices along [001]. In cases where they are, as in lalondeite, double layers, $T_2\overline{T}_2$, of composition $T_{16}O_{38}$ are formed. These double layers produce large channels within which ions of large radius (K,Na) and H_2O can be accommodated. In situations where the double layers are not condensed, as in gyrolite, an interlayer component containing ions of large radius coordinated by H_2O is formed. Such interlayer components can be highly variable in terms of thickness and content, and can play important roles in the indus-

FIG. 3. The $OT_2\overline{T}_2O$ module in lalondeite. The six-membered silicate rings (light green tetrahedra) are cross-linked by *Si*3O$_4$ (orange) and *Si*6O$_4$ (blue) tetrahedra. The closest-packed *O* layer is composed of NaO$_6$ (purple) and CaO$_6$ (blue) octahedra. The H_2O molecules are shown as green spheres, and the disordered *Na*2a,b ions, as red spheres.

TABLE 5. EMPIRICAL BOND-VALENCE SUMS (*vu*) FOR LALONDEITE*

	Na1	Na2a†	Na2b†	Ca1	Ca2	Ca3†	Si1	Si2	Si3	Si4	Si5	Si6	Si7	Si8	ΣV
O1	0.135			$0.318^{\times 2}$		0.307					1.157				1.917
O2					0.336	0.204 0.178							1.189		1.907
O3		0.059	0.026				1.000	1.000							2.085
O4									1.067			1.126			2.193
O5				$0.319^{\times 2}$	0.336	0.147		1.067							1.869
O6	0.115				0.365 0.322					1.117					1.919
O7		0.068	0.040								0.981			0.981	2.070
O8	0.130			$0.346^{\times 2}$	0.302		1.189								1.967
O9	0.125				0.336	0.222								1.189	1.872
O10							0.971		1.027						1.998
O11		0.066	0.033							0.989			0.968		2.056
O12									1.047		0.958				2.005
O13										1.039		1.014			2.053
O14								0.981				1.030			2.011
O15	0.038	0.044	0.023							1.000	1.027				2.132
O16									1.070				0.958		2.028
O17												1.041		1.011	2.052
O18		0.066	0.034				0.992							0.987	2.079
O19		0.064	0.023					1.005					1.022		2.114
F	$0.158^{\times 2}$	0.077				0.234									0.627
ΣV	0.859	0.444	0.189	1.966	1.997	1.292	4.152	4.053	4.211	4.145	4.123	4.211	4.137	4.168	

* Parameters from Brese & O'Keeffe (1991). † Calculated using refined site-occupancy factors.

TABLE 6. CRYSTALLOGRAPHY, CHEMICAL FORMULAE AND STRUCTURAL SCHEME FOR MEMBERS OF THE REYERITE–GYROLITE GROUP AND RELATED SYNTHETIC PHASES

Mineral	Crystal-chemical formula	Space group	*a* (Å)	*b*	*c*	α (°)	β	γ	Structural scheme
Fedorite [1]	$(Na,K)_{2-3}(Ca,Na)_7(Si,Al)_{16}O_{38}F_2{\bullet}3\text{-}4H_2O$	$P\overline{1}$	9.6450	9.6498	12.6165	102.427	96.247	119.894	$OT_2\overline{T}_2O$
K Phase [2]	$Ca_7Si_{16}O_{38}(OH)_2$	$P\overline{1}$	9.70	9.70	12.25	108.5	78.0	120.0	$OT_2\overline{T}_2O$
Lalondeite [3]	$(Na,Ca,\square)_6Ca_3Si_{16}O_{38}(F,OH)_2{\bullet}3H_2O$	$P\overline{1}$	9.589	9.613	12.115	96.62	92.95	119.81	$OT_2\overline{T}_2O$
Reyerite [4]	$(Na,K)_2Ca_{14}Si_{22}Al_2O_{58}(OH)_8{\bullet}6H_2O$	$P\overline{3}$	9.765			19.067			$T_1OT_2\overline{T}_2\overline{O}T_1$
Truscottite [5]	$(Ca,Mn)_{14}Si_{14}O_{58}(OH)_8{\bullet}2H_2O$	$P\overline{3}$	9.735			18.83			$T_1OT_2\overline{T}_2\overline{O}T_1$
Martinite [6]	$(Na,\square,Ca)_{12}Ca_4(Si,S,B)_{14}B_2O_{38}(OH,Cl)_2F_2{\bullet}4H_2O$	$P\overline{1}$	9.5437	9.5349	14.0268	108.943	74.154	119.780	$OT_2X\overline{T}_2O$
Z Phase [7]	$Ca_9Si_{16}O_{40}(OH)_2{\bullet}(14+x)H_2O$	?	9.65	9.65	15.3	?	?	120.0	$OT_2X\overline{T}_2O$
Gyrolite [8]	$Ca_{16}NaSi_{23}AlO_{60}(OH)_8{\bullet}14H_2O$	$P\overline{1}$	9.74	9.74	22.40	95.7	91.5	120.0	$T_1OT_2X\overline{T}_2\overline{O}T_1$
Tungusite [9]	$Ca_{14}Fe^{2+}{}_9Si_{24}O_{60}(OH)_{22}$	$P\overline{1}$	9.714	9.721	22.09	90.13	98.3	120.0	$T_1OT_2X\overline{T}_2\overline{O}T_1$
Orlymanite [10]	$Ca_4Mn_3Si_8O_{20}(OH)_6{\bullet}2H_2O$	$P3$ or $P\overline{3}$	9.60		35.92				$T_1O\overline{T}_1\overline{O}T_2$ $OT_1\overline{O}T_1$ (?)

References: 1) Mitchell & Burns (2001), 2) Gard *et al.* (1981), 3) this study, 4) Merlino (1988), 5, Lachowski *et al.* (1979), 6) McDonald & Chao (2007), 7) Gard *et al.* (1975), 8) Merlino (1988), 9) Ferraris *et al.* (1995), 10. Peacor *et al.* (1990).

trial applications of these minerals (and their related synthetic counterparts) as they are expandable and, in some cases, the expansion is reversible (*e.g.*, gyrolite; Garbev *et al*. 2004).

The *T*, *O* and *X* structural components in reyerite-group minerals are arranged in a variety of ways to create modules that are stacked perpendicular to [001]; in this regard, they possess crystal structures reminiscent of those found in typical phyllosilicates. For example, the crystal structure of reyerite may be described as having a $T_1OT_2\overline{T}_2\overline{O}T_1$ module (Table 6). Within the reyerite–gyrolite group, there is a spectrum of crystal-structure complexity, progressing from a structure like that of lalondeite with the simplest module (one *T* and one *O* layer and no continuous interlayer component), to gyrolite (Table 6). Using the terminology of Merlino (1988) and the modification proposed by McDonald & Chao (2007), lalondeite can be described as having a $OT_2\overline{T}_2O$ module.

Genetic Implications

As discussed by McDonald & Chao (2007), minerals of the reyerite–gyrolite group are generally interpreted to be late-stage phases produced through low-temperature hydrothermal alteration or metamorphism of mafic rocks (usually alkali basalts). In many cases, they occur in vugs along with assemblages that include other hydrated, low-temperature minerals. Synthetic equivalents of members of this group constitute important phases in the cement industry; hence numerous studies of conditions of their formation have been undertaken (Taylor 1997). In general, these investigations have demonstrated that at low temperature (*i.e.,* ~100°C), poorly ordered gels exist, but as temperature increases (200–250°C), ordering occurs, possibly through a continuous, diffusion-controlled mechanism involving the silicate layers (Shaw *et al*. 2002). This process of ordering ultimately leads to the formation of phases equivalent to some reyerite–gyrolite-group minerals (*e.g.*, truscottite). Although a complete knowledge regarding its mode of occurrence is lacking, there is a strong suggestion that like other members of the group, lalondeite is a low-temperature phase, possibly forming as a result of ordering of a precursor, gel-like material.

Acknowledgements

Our sincere thanks to Dr. J. Szymánski (formerly of CANMET) for assistance with the four-circle diffractometer, Mr. D. Crabtree (Ontario Geoscience Laboratory) for help with electron-microprobe analyses, Mr. J. Poulin for alerting the first author to the fluorescence of lalondeite under medium-wave radiation, and Dr. P. Tarassoff for discussions regarding the occurrence of the mineral. Mr. Laszló Horváth contributed the photographs. We are also most grateful to the reviewers, John B. Higgins, Stuart J. Mills, and Associate Editor Carl A. Francis, for their constructive comments and recommendations. Financial support, provided through a grant to AMM from the Natural Sciences and Engineering Research Council, is gratefully acknowledged.

References

Bonaccorsi, E. & Merlino, S. (2005): Modular microporous minerals: cancrinite–davyne group and C–S–H phases. *In* Micro- and Mesoporous Mineral Phases (G. Ferraris & S. Merlino, eds.). *Rev. Mineral. Geochem.* **57**, 241-290.

Brese, N.E. & O'Keeffe, M. (1991): Bond-valence parameters for solids. *Acta Crystallogr.* **B47**, 192-197.

Cromer, D.T. & Liberman, D. (1970): Relativistic calculation of anomalous scattering factors for X rays. *J. Chem. Phys.* **53**, 1891-1898.

Cromer, D.T. & Mann, J.B. (1968): X-ray scattering factors computed from numerical Hartree–Fock wave functions. *Acta Crystallogr.* **A24**, 321-324.

Farmer, V.C. (1974): The *Infrared Spectra of Minerals*. The Mineralogical Society, London, U.K. (Monogr. **4**).

Ferraris, G., Pavese, A. & Soboleva, S.V. (1995): Tungusite: new data, relationship with gyrolite and structural model. *Mineral. Mag.* **59**, 535-543.

Gabe, E.J., Le Page, Y., Charland, J.-P., Lee, F.L. & White, P.S. (1989): NRCVAX – an interactive program system for structural analysis. *J. Appl. Crystallogr.* **22**, 384-387.

Garbev, K., Black, L., Stumm, A., Stemmermann, P. & Basharova, B. (2004): Polymerization reactions by thermal treatment of gyrolite-group minerals – an IR spectroscopic and X-ray diffraction study based on synchrotron radiation. *In* Proc. 8th Int. Congress on Applied Mineralogy (M. Pecchio, F.R.D. Andrade, L.Z. D'Agostino, H. Kahn, L.M. Sant'Agostino & M.M.M.L. Tassinari, eds.). *International Council for Applied Mineralogy of Brasil* (ICAM–BR), 245-248.

Gard, J.A., Luke, K. & Taylor, H.F.W. (1981): The crystal structure of K-phase. *Kristallographia* **26**, 1218-1223.

Gard, J.A., Mitsuda, T. & Taylor, H.F.W. (1975): Some observations on Assarson's Z-phase and its structural relations to gyrolite, truscottite, and reyerite. *Mineral. Mag.* **40**, 325-334.

Lachowski, E.E., Murray, L.W. & Taylor, H.F.W. (1979): Truscottite: composition and ionic substitutions. *Mineral. Mag.* **43**, 333-336.

Mandarino, J.A. (1981): The Gladstone–Dale relationship. IV. The compatibility concept and its application. *Can. Mineral.* **19**, 441-450.

MCDONALD, A.M. & CHAO, G.Y. (2007): Martinite, a new hydrated sodium calcium fluorborosilicate species from Mont Saint-Hilaire, Quebec: description, structure determination and genetic implications. *Can. Mineral.* **45**, 1281-1292.

MERLINO, S. (1988): Gyrolite: its crystal structure and crystal chemistry. *Mineral. Mag.* **52**, 377-387.

MITCHELL, R.H. & BURNS, P.C. (2001): The structure of fedorite: a re-appraisal. *Can. Mineral.* **39**, 769-777.

NOLZE, G. & KRAUS, W. (1998): POWDERCELL, *v*. 2.3. Federal Institute for Materials Research and Testing, Berlin, Germany.

PEACOR, D.R., DUNN, P.J. & NELEN, J.A. (1990): Orlymanite, $Ca_4Mn_3Si_8O_{20}(OH)_6•2H_2O$, a new mineral from South Africa: a link between gyrolite-family and conventional phyllosilicate minerals? *Am. Mineral.* **75**, 923-927.

SHAW, S.M., HENDERSON, C.M.B. & CLARK, S.M. (2002): In-situ synchrotron study of the kinetics, thermodynamics, and reaction mechanisms of the hydrothermal crystallization of gyrolite, $Ca_{16}Si_{24}O_{60}(OH)_8•14H_2O$. *Am. Mineral.* **87**, 533-541.

SHELDRICK, G.M. (1993): SHELXL–93: *a Program for the Refinement of Crystal Structures*. Univ. of Göttingen, Göttingen, Germany.

TAYLOR, H.F.W. (1997): *Cement Chemistry* (2nd ed.). Academic Press, London, U.K.

WIGHT, Q. & CHAO, G.Y. (1995): Mont St-Hilaire revisited. *Rocks & Minerals* **61**, 182-197.

Received August 27, 2008, revised manuscript accepted January 28, 2009.